CERN-PH-TH/2007-035
LU TP 07-05
hep-ph/0702170

The Hadronic Light-by-Light Contribution to the Muon Anomalous Magnetic Moment: Where Do We Stand?

Johan Bijnens[a)] **and Joaquim Prades**[b)] [a]

[a)] Department of Theoretical Physics, Lund University
Sölvegatan 14A, S-22362 Lund, Sweden.

[b)] Theory Unit, Physics Department, CERN
CH-1211 Genève 23, Switzerland.

We review the status of the hadronic light-by-light contribution to the muon anomalous magnetic moment and critically compare recent calculations. We also study in detail which momentum regions the π^0 exchange main contribution originates. We also argue that $a_\mu^{light-by-light} = (11 \pm 4) \times 10^{-10}$ encompasses the present understanding of this contribution and comment on some directions to improve on that.

February 2007

[a]On leave of absence from CAFPE and Departamento de Física Teórica y del Cosmos, Universidad de Granada, Campus de Fuente Nueva, E-18002 Granada, Spain.

Modern Physics Letters A

The Hadronic Light-by-Light Contribution to the Muon Anomalous Magnetic Moment: Where Do We Stand?

JOHAN BIJNENS
Department of Theoretical Physics, Lund University,
Sölvegatan 14A, SE 22362 Lund, Sweden
bijnens@thep.lu.se

JOAQUIM PRADES*
Theory Unit, Physics Department, CERN
CH-1211 Genève 23, Switzerland
prades@ugr.es

Received (Day Month Year)
Revised (Day Month Year)

We review the status of the hadronic light-by-light contribution to the muon anomalous magnetic moment and critically compare recent calculations. We also study in detail which momentum regions the π^0 exchange main contribution originates. We also argue that $a_\mu^{light-by-light} = (11 \pm 4) \times 10^{-10}$ encompasses the present understanding of this contribution and comment on some directions to improve on that.

Keywords: Muon; Anomalous magnetic moment

PACS Nos.: 13.40.Em; 11.15.Pg; 12.20.Fv; 14.60.Ef

1. Introduction

The muon anomalous magnetic moment $g-2$ [$a_\mu \equiv (g-2)/2$] has been measured by the E821 experiment (Muon g-2 Collaboration) at Brookhaven National Laboratory (BNL) with an impressive accuracy of 0.72 ppm [1] yielding the present world average[1]

$$a_\mu^{\rm exp} = 11\,659\,208.0(6.3) \times 10^{-10} \tag{1}$$

with an accuracy of 0.54 ppm. New experiments[2,3] are under design with a goal of measuring a_μ with an accuracy of at least 0.25 ppm.

On the theory side, a large amount of work has been devoted to reduce the uncertainty of the Standard Model prediction. A recent updated discussion with an extensive list of references for both theoretical predictions and experimental results

*On leave of absence from CAFPE and Departamento de Física Teórica y del Cosmos, Universidad de Granada, Campus de Fuente Nueva, E-18002 Granada, Spain.

is Ref. 3 and Ref. 4, and a more introductory exposition can be found in the lectures by Knecht in Ref. 5.

In this paper, we review the present status of the hadronic light-by-light contribution (hLBL). A somewhat shorter version is the published talk in Ref. 6. The uncertainty in the hLBL is expected to eventually become the largest theoretical error. This contribution is shown schematically in Fig. 1. It consists of three photon legs coming from the muon line connected to the external electromagnetic field by hadronic processes. Its contribution can be written as

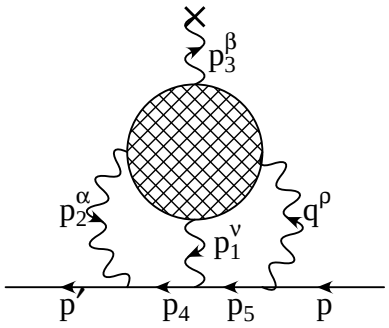

Fig. 1. The hadronic light-by-light contribution to the muon $g-2$.

$$\mathcal{M} = |e|^7 V_\beta \int \frac{\mathrm{d}^4p_1}{(2\pi)^4} \int \frac{\mathrm{d}^4p_2}{(2\pi)^4} \frac{1}{q^2\, p_1^2\, p_2^2 (p_4^2-m^2)\,(p_5^2-m^2)} \times \Pi^{\rho\nu\alpha\beta}(p_1,p_2,p_3)\, \bar{u}(p')\gamma_\alpha(\not{p}_4+m)\gamma_\nu(\not{p}_5+m)\gamma_\rho u(p) \tag{2}$$

where $q=p_1+p_2+p_3$. To obtain the amplitude $\mathcal{M}$ in (2), the hadronic contribution to the full correlator $\Pi^{\rho\nu\alpha\beta}(p_1,p_2,p_3\to 0)$ needs to be known for all possible four-momenta p_1 and p_2. The correlator is defined via

$$\Pi^{\rho\nu\alpha\beta}(p_1,p_2,p_3) = i^3 \int \mathrm{d}^4x \int \mathrm{d}^4y \int \mathrm{d}^4z e^{i(p_1\cdot x+p_2\cdot y+p_3\cdot z)} \times \langle 0|T\left[V^\rho(0)V^\nu(x)V^\alpha(y)V^\beta(z)\right]|0\rangle \tag{3}$$

with $V^\mu(x) = \left[\overline{q}\hat{Q}\gamma^\mu q\right](x)$ and $\hat{Q} = \mathrm{diag}(2,-1,-1)/3$ the quark charges. The external magnetic field couples to the photon leg with momentum $p_3\to 0$. In the remainder whenever we refer to a_μ we specifically mean only the hadronic light-by-light contribution to it.

Clearly, the correlator (3) is a complicated object. It contains many independent Lorentz structures, each of comes with a function of the variables p_1^2, p_2^2 and q^2. As a consequence, many different energy scales can be involved in the calculation of the hadronic light-by-light contribution to muon $g-2$. This makes it difficult to obtain the full needed behavior of the correlator (3) from known constraints. Therefore

no full first principles calculation exists at present. The needed results cannot be directly related to measurable quantities either. Lattice QCD calculations are at the exploratory stage only, see e.g. Ref. 7.

In fact, there has long been a confusion about hadronic exchanges[a] versus quark loop estimates. This confusion was resolved by organizing the different contributions according to the lowest power in $1/N_c$ and the lowest order in the chiral perturbation theory (CHPT) expansion counting where they start contributing[9]. One can distinguish four types of contributions:

- Goldstone boson exchange contributions are order N_c and start contributing at order p^6 in CHPT.
- (Constituent) quark-loop and non-Goldstone boson exchange contributions are order N_c and start contributing at order p^8 in CHPT.
- Goldstone boson loop contributions are order one in $1/N_c$ and start contributing at order p^4 in CHPT.
- Non-Goldstone boson loop contributions are order one in $1/N_c$ and start to contribute at order p^8 in CHPT.

The two existing *full* calculations[8,10], are based on this classification. The Goldstone boson exchange contribution (GBE) was shown to be numerically dominant in Refs. 8 and 10 after strong cancellations between the other contributions. But the other contributions, though each smaller than the GBE, were not separately negligible. Using effective field theory techniques, Ref. 11 showed that the leading double logarithm comes from the GBE and was positive. Refs. 11 and 12 found a global sign mistake in the GBE of the earlier work[8,10] which was confirmed by the authors of those works[13,14] and by others[15,16]. In the remainder we will always correct for this sign mistake without explicitly mentioning it.

Recently, Melnikov and Vainshtein pointed out new short-distance constraints on the correlator (3) in Ref. 17, studied and extended in Ref. 18. The authors of Ref. 17 constructed a model which satisfies their main new short-distance constraints in order to study its effects and found a number significantly different from the earlier work. They approximated the full hLBL by the GBE and axial-vector exchange contributions.

One of the purposes of this review is to critically compare the different contributions in the different calculations and extend somewhat on our earlier comments[6]. For the dominant GBE we also present some new results on the momentum regions which are relevant. In earlier work several studies were done to check which momentum regions were important. These used different methods, varying the vector meson mass[10], studying the cut-off dependence[8] and expansions around various momentum regions in the loop integrals[17,19].

In Sect. 2 we discuss the calculations done before 2002 and compare their results.

[a]We stick here to the formulation "exchange" as used by us[8]. It is often referred to as "pole" contributions. We consider this misleading because the exchanged particle is used off-shell.

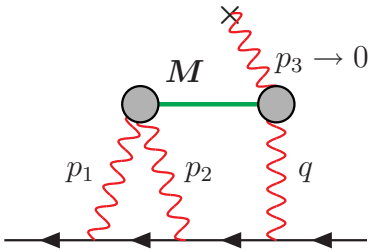

Fig. 2. A generic meson exchange contribution to the hadronic light-by-light part of the muon $g-2$.

Sect. 3 discusses the short distance constraints proposed by Melnikov and Vainshtein and the numerical results presented in their paper. In Sect. 4 we show in detail in which momentum regions the contributions from π^0 exchange originate and Sect. 5 compares and comments on the various contributions in the different calculations. Finally, we present our conclusions as to the present best value and error for the hLBL in Sect. 6.

2. Results obtained up to 2002

In this section we discuss the calculations performed in the period 1995-2001. These were organized according to the large N_c and CHPT countings [9] discussed above. The CHPT counting is used as a classification tool, none of these calculations were actually performed at a fixed order in CHPT. We want to emphasize once more that the calculations in Refs. 8, 10, 13 and 14 showed that only after several large cancellations in the rest of the contributions, the numerically dominant one is the Goldstone boson exchange. In this section we concentrate on the work in Refs. 8 and 13, with some comments and results from Refs. 10, 12 and 14.

2.1. *Pseudo-Scalar Exchange*

The pseudo-scalar exchange was saturated by the Goldstone boson exchange in Refs. 8, 10, 13 and 14. This contribution is shown in Fig. 2 with $M = \pi^0, \eta, \eta'$.

Refs 8 and 13, used a variety of $\pi^0\gamma^*\gamma^*$ form factors

$$\mathcal{F}^{\mu\nu}(p_1,p_2) \equiv N_c/(6\pi)\,(\alpha/f_\pi)\,i\,\varepsilon^{\mu\nu\alpha\beta}p_{1\alpha}p_{2\beta}\,\mathcal{F}(p_1^2,p_2^2) \tag{4}$$

fulfilling several possible QCD constraints. A more extensive analysis of this form factor was done in Ref. 20 finding very similar numerical results. In particular, the three-point form factors $\mathcal{F}(p_1^2,p_2^2)$ used in Refs. 8 and 13 had the correct QCD

Table 1. Results for the π^0 and π^0, η and η' exchange contributions.

	$10^{10} \times a_\mu$	
	π^0 only	π^0, η and η'
Bijnens, Pallante and Prades [8,13]	5.6	8.5 ± 1.3
Hayakawa and Kinoshita [10,14]	5.7	8.3 ± 0.6
Knecht and Nyffeler [12] ($h_2 = 0$)	5.8	8.3 ± 1.2
Knecht and Nyffeler [12] ($h_2 = -10$ GeV^2)	6.3	
Melnikov and Vainshtein [17]	7.65	11.4±1.0

Table 2. Results for the axial-vector exchange contributions.

Axial-Vector Exchange Contributions	$10^{10} \times a_\mu$
Bijnens, Pallante and Prades [8,13]	0.25 ± 0.10
Hayakawa and Kinoshita [10,14]	0.17 ± 0.10
Melnikov and Vainshtein [17]	2.2±0.5

short-distance behavior[b]

$$\mathcal{F}(Q^2, Q^2) \to A/Q^2\,, \quad \mathcal{F}(Q^2, 0) \to B/Q^2\,, \tag{5}$$

when Q^2 is Euclidean. These form factors were in agreement with available data including the slope at the origin as well as treating the π^0, η and η' mixing. All form factors converged for a cutoff scale $\Lambda \sim (2-4)$ GeV and produced small numerical differences when plugged into the hadronic light-by-light contribution.

Somewhat different $\mathcal{F}(p_1^2, p_2^2)$ form factors where used in Refs. 10, 12 and 14 but the results agree well. For comparison, one can find the results of Refs. 8, 10, 12, 13 and 14 in Tab. 1 of the π^0 exchange and after adding η and η' exchange contributions to the dominant π^0 one.

2.2. *Axial-Vector Exchange*

This contribution is depicted in Fig. 2 with $M = A = a_1^0, f_1$ and possibly other axial-vector resonances. For this contribution one needs the $A\gamma\gamma^*$ and $A\gamma^*\gamma^*$ form factors. Little is known about these but there exist anomalous Ward identities which relate them to the $P\gamma\gamma^*$ and $P\gamma^*\gamma^*$ form factors.

This contribution was not studied by Knecht and Nyffeler[12]. Refs. 8, 10, 13 ands 14 used nonet symmetry, which is exact in the large N_c limit, for the masses of the axial-vector resonances. Their results are shown in Tab. 2 for comparison.

[b] The observance of QCD short-distance constraints was implemented for this one and several other contributions in Refs. 8 and 13, contrary to the often heard wrong claim that Ref. 17 is the first calculation to take such constraints into account, e.g. see Ref. 21.

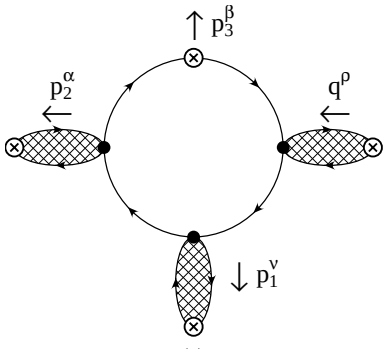

Fig. 3. Quark-loop contribution, as modeled in ENJL.

2.3. *Scalar Exchange*

This contribution is shown in Fig. 2 with $M = S = a_0, f_0$ and possible other scalar resonances. For this contribution one needs the $S\gamma\gamma^*$ and $S\gamma^*\gamma^*$ form factors. Within the extended Nambu–Jona-Lasinio (ENJL) model used in Refs. 8 and 13, chiral Ward identities impose relations between the constituent quark loop and scalar exchanges. The needed scalar form factors are also constrained at low energies by CHPT. Refs. 8 and 13 used nonet symmetry for the masses. This contribution was not included by the other groups[10,14,17].

The leading logarithms of the scalar exchange are the same as those of the pion exchange but with opposite sign[15]. Refs. 8 and 13 find that sign for the full scalar exchange contribution, obtaining

$$a_\mu(\text{Scalar}) = -(0.7 \pm 0.2) \times 10^{-10}\,. \tag{6}$$

2.4. *Other contributions at leading order in $1/N_c$.*

This includes any contributions that are not modeled by exchanged particles. At short-distance, the main one is the quark-loop. At long distances they are often modeled as a constituent quark-loop with form factors in the couplings to photons. This corresponds to the contribution shown in Fig. 3. Refs. 8 and 13 split up the quark momentum integration into two pieces by introducing an Euclidean matching scale Λ. At energies below Λ, the ENJL model was used to compute the quark-loop contribution while above Λ a bare (partonic) heavy quark loop of mass Λ was used. The latter part scales as $1/\Lambda^2$ and mimics the high energy behavior of QCD for a massless quark with an IR cut-off around Λ –see footnote [b]. Adding these two contributions yields a stable result as can be seen in Tab. 3.

2.5. *NLO in $1/N_c$: Goldstone Boson Loops*

At next-to-leading order (NLO) in $1/N_c$, the leading contribution in the chiral counting to the correlator in (2), corresponds to charged pion and Kaon loops

Table 3. Sum of the short- and long-distance quark loop contributions[8] as a function of the matching scale Λ.

Λ [GeV]	0.7	1.0	2.0	4.0
$10^{10} \times a_\mu$	2.2	2.0	1.9	2.0

Table 4. Results for the charged and Kaon loop contributions to the hadronic light-by-light contribution to muon $g-2$.

Charged Pion and Kaon Loop Contributions	$10^{10} \times a_\mu$
Bijnens, Pallante and Prades (Full VMD) [8,13]	-1.9 ± 0.5
Hayakawa and Kinoshita (HGS) [10,14]	-0.45 ± 0.85
Melnikov and Vainshtein (Full NLO in $1/N_c$ guess) [17]	0 ± 1

which can be depicted analogously to the quark-loop in Fig. 3 but with charged pions and Kaons running inside the loop instead. In general one expects loops of heavier particles to be suppressed and has only been evaluated for the pion loop and the much smaller Kaon loop.

The needed form factors[c] $\gamma^* P^+ P^-$ and $\gamma^*\gamma^* P^+ P^-$ vertices were studied extensively in Ref. 8. In particular which form factors were fully compatible with chiral Ward identities were studied. The full vector meson dominance model (VMD) is one model fulfilling the known constraints. The conclusion unfortunately is that there is a large ambiguity in the momentum dependence starting at order p^6 in CHPT. Both the full VMD model[8,13] and the hidden gauge symmetry (HGS) model[10,14] satisfy the known constraints. Unfortunately, this ambiguity cannot easily be resolved since there is no data for $\gamma^*\gamma^* \to \pi^+\pi^-$. Adding the charged pion and Kaon loops, the results obtained in Refs. 8 and 10 are listed in Tab. 4.

In view of this model dependence, the authors of Refs. 8 and 13 considered that the difference between the results from Ref. 8 and Ref. 10 for this contribution needs to be added *linearly* to the final uncertainty of the hadronic light-by-light contribution to a_μ.

3. New Short-Distance Constraints

Melnikov and Vainshtein pointed out[17] a new short-distance constraint on the correlator (3). This constraint is for

$$\langle T[V^\nu(p_1)V^\alpha(p_2)V^\rho(-q=-p_1-p_2)]|\gamma(p_3\to 0)\rangle \tag{7}$$

[c]Note that neither the ENJL model nor any fixed order in CHPT was used in any of the estimates of this contribution.

Table 5. Results quoted in Ref. 17 for the pseudo-vector exchange depending of the $f_1(1285)$ and $f_1(1420)$ resonances mass mixing.

Mass Mixing	$10^{10} \times a_\mu$
No OPE and Nonet Symmetry with M=1.3 GeV	0.3
New OPE and Nonet Symmetry with M= 1.3 GeV	0.7
New OPE and Nonet Symmetry with M= M_ρ	2.8
New OPE and Ideal Mixing with Experimental Masses	2.2 ± 0.5

and follows from the OPE for two vector currents when $P_1^2 \simeq P_2^2 \gg Q^2$ with $P_1^2 = -p_1^2$, $P_2^2 = -p_2^2$ and $Q^2 = -q^2$:

$$T[V^\nu(p_1)V^\alpha(p_2)] \sim \varepsilon^{\nu\alpha\mu\beta}\,(\hat{p}_\mu/\hat{p}^2)\,[\overline{q}\hat{Q}^2\gamma_\beta\gamma_5 q](p_1+p_2) \tag{8}$$

with $\hat{p} = (p_1 - p_2)/2 \simeq p_1 \simeq -p_2$ and $\hat{Q}$ is the light quark electrical charge matrix (3). This constraint was afterward generalized in Ref. 18. Note that the new part is the use of (8) for the full correlator (3). Short-distance was already used to obtain the first constraint in (5).

The authors of Ref. 17 saturated the full correlator by exchanges. The new OPE constraint is satisfied by introducing a pseudo-scalar exchange with the vertex on the q, p_3 side of Fig. 2 point-like rather than including a form factor. This change strongly breaks the symmetry between the two ends of the exchanged particle. There are also OPE constraints for $P_1^2 \approx P_2^2 \approx Q^2$ and $P_2^2 \approx Q^2 \gg P_1^2$, essentially derived from the quark-loop behavior in this regime[17]. Both latter OPE constraints on the correlator (3) are not satisfied by the model used in Ref. 17 but they argued that this made only a small numerical difference of order 0.05×10^{-10}.

Ref. 17 added to the pseudo-scalar exchange an axial-vector exchange contribution. They found this contribution to be extremely sensitive to the mixing of the resonances $f_1(1285)$ and $f_1(1420)$ as can be seen in Tab. 5, taken from the results there. The difference between the lines labeled "No OPE" and "New OPE" is the effect of making the q, p_3 vertex point-like. The authors of Ref. 17 took the ideal mixing result for their final result for a_μ.

4. Momentum Regions for π^0 Exchange

We were somewhat puzzled by the effect when saturating the new short distance constraint by GBE in Ref. 17 and have therefore done a few studies to see whether the changes there come from large momentum regimes or are located elsewhere. This was because our total estimate of the quark-loop was similar to the numerical change in the GBE of Ref. 17. In order to do this study, we have adapted the method used in Refs. 8 and 20 to various form factors used in earlier works. We rotate the integrals in (2) into Euclidean space. The eight dimensional integral can be easily reduced to a five dimensional integral. Here one can choose as variables[d] P_1, P_2 and

[d]In Refs. 8 and 20 a different set was used not quite as suitable for the present study.

Table 6. π^0-exchange results for $10^{10} \times a_\mu$ with a cut-off on the three photon momenta for the four cases described in the text. The last column is the difference between MV and KN form factors. The numerical error is at or below the last digit quoted.

Cut-off Λ (GeV)	WZW	VMD	KN	MV	MV−KN
0.5	4.74	3.37	3.39	3.68	0.29
0.7	7.51	4.41	4.47	5.01	0.54
1.0	11.3	5.14	5.29	6.15	0.86
2.0	21.9	5.60	5.99	7.34	1.35
4.0	33.8	5.65	6.20	7.79	1.59
8.0	49.6	5.65	6.24	7.92	1.69
16.0	68.	5.64	6.23	7.96	1.73

Q and two angles θ_1 and θ_2. These are the angles between the Euclidean p_1, p_2 and the muon momentum while P_1, P_2 and Q are the size of the Euclidean momenta with $P_1^2 = -p_1^2$, $P_2^2 = -p_2^2$ and $Q^2 = -q^2$. Ref. 12 performed the integrals over three of these quantities analytically but not for the asymmetric case used by Ref. 17. We have therefore use numerical integration. The main integration routine used by us earlier[8,20] was VEGAS. For the present study we have also performed the integration using an adaptive Gaussian multidimensional integration routine and have checked for several quantities that both agree and reproduce earlier known results.

We will show the contributions to the muon anomalous magnetic moment from π^0 exchange for several different form factors. These correspond to the point-like $\pi^0\gamma^*\gamma^*$ form factor (WZW), the full vector meson dominance model (VMD), the LMD+V form factor[12] with $h_2 = -10$ GeV^2 (KN) and the latter form factor but with the point-like version on the soft-photon end[17] (MV). We will refer to these form factors as WZW, VMD, KN, and MV in the remainder of this section. We have used the values $h_1 = 0, h_5 = 6.93$ GeV^2 and the value of h_7 as given by Ref. 12. We picked the value of h_2 that was argued[17] to better produce subleading OPE constraints. It raises the central value somewhat compared to $h_2 = 0$ as shown in Tab. 1

As inputs we used $M_V = M_{V_1} = 0.770$ GeV and $M_{V_2} = 1.465$ GeV, $F_\pi = 92.4$ MeV and the measured π^0 and muon masses. This is the origin of the minor differences with Ref.12.

As a first indication where the contributions to a_μ come from, we have listed in Tab. 6 the value of a_μ for the four cases with the constraint $Q, P_1, P_2 < \Lambda$. We have shown the logarithmically square divergent point-like case here to show the size of the suppression introduced by the form factors. Note that we cannot reproduce the 7.65 of Ref. 17 but we do reproduce the results of Refs. 8, 12 and 20. The new short-distance constraint (8) came from the region $Q \ll P_1 \approx P_2$. We have thus checked how much of the difference and total comes from the region with $Q < \min(P_1, P_2)$ and from the region with Q larger than at least one of (P_1,P_2), the numbers quoted

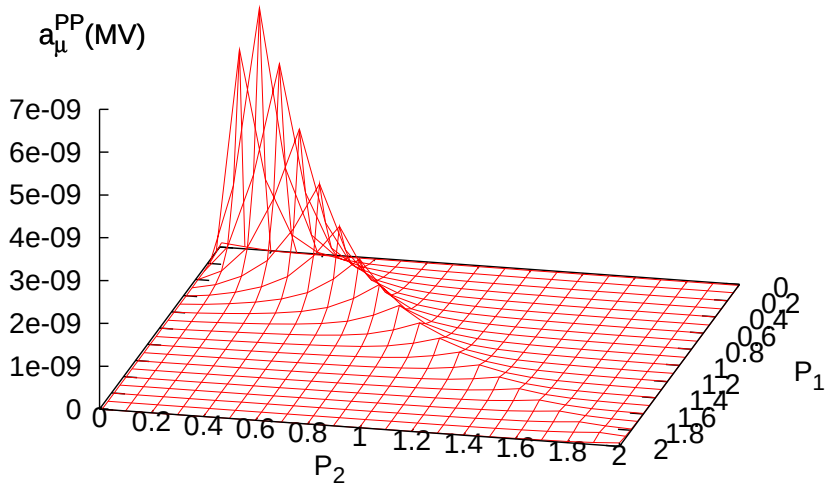

Fig. 4. The quantity a_μ^{PP} of Eq. 10) as a function of P_1 and P_2 for the MV choice.

are for $\Lambda = 16$ GeV. The numbers are $10^{10} \times a_\mu$.

$$\begin{array}{lllll} Q < \min(P_1, P2): & 4.01\ (\mathrm{KN}) & 4.74\ (\mathrm{MV}) & 0.73\ (\mathrm{MV}{-}\mathrm{KN}) \\ Q > \min(P_1, P_2): & 2.24\ (\mathrm{KN}) & 3.23\ (\mathrm{MV}) & 0.99\ (\mathrm{MV}{-}\mathrm{KN}) \end{array} \tag{9}$$

As one sees, in fact, most of the difference comes from the region where the OPE condition is strongly violated.

The results in Tab. 6 give only a partial indication of which momentum regions are important. In the remaining figures we therefore show the contribution to a_μ in several ways. We always denote p_1, p_2 as the momenta on the π^0 side with both photons connected to the muon line and q the momentum on the soft-photon side. We can thus rewrite the contribution to a_μ of (2) in various ways:

$$\begin{aligned} a_\mu &= \int dP_1 dP_2\ a_\mu^{PP}(P_1, P_2) \\ &= \int dl_1 dl_2\ a_\mu^{LL}(l_1, l_2) \\ &= \int dl_1 dl_2 dl_q\ a_\mu^{LLQ}(l_1, l_2, l_q)\,, \end{aligned}$$
$$\text{with} \quad l_1 = \log(P_1/\mathrm{GeV}), \quad l_2 = \log(P_2/\mathrm{GeV}), \quad \text{and} \quad l_q = \log(Q/\mathrm{GeV})\,. \tag{10}$$

In Fig. 4 we have plotted $10^{10} \times a_\mu^{PP}(P_1, P_2)$ as a function of P_1 and P_2. In this way of plotting it is however rather difficult to see why the contribution with at least one scale above 1 GeV is as large as shown in Tab. 6. The quantity a_μ^{LL} is much more suitable for this. The result for a_μ after integrating for this quantity is directly proportional to the volume under the surface as it is plotted in Figs. 5, 6

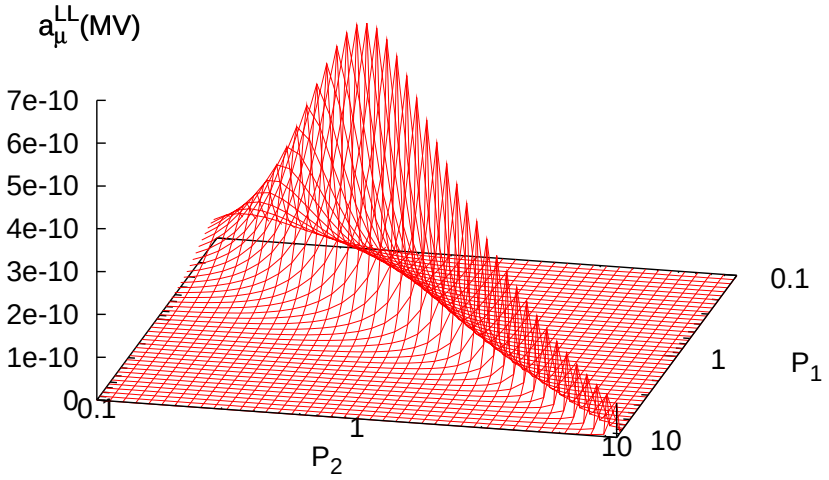

Fig. 5. The quantity a_μ^{LL} of Eq. 10) as a function of P_1 and P_2 for the MV choice. a_μ is directly related to the volume under the surface as plotted.

and 7 with a logarithmic scale for P_1 and P_2. We have used the same scale for all three plots. What one finds is that the VMD one has much smaller contributions for P_1 and P_2 large but both MV and KN show a significant contribution even at fairly high values of (P_1, P_2). Also the contribution at these higher values of (P_1, P_2) is concentrated along the axis $P_1 = P_2$. One also see by comparing Figs. 5 and 6 that the enhancement of the MV result over the KN result comes not from a very different shape but more a general increase over the entire region. The parts below 0.1 GeV were not plotted, these are very similar for all three cases. A plot for the WZW case simply shows a constantly growing ridge along $P_1 = P_2$ which produces then the $\log^2 \Lambda$ divergence.

The figures before give an indication of which ranges of (P_1, P_2) are important. But what about the values of Q that are relevant. This will of course depend on the values of P_1 and P_2. We show in Fig. 8 the value for a_μ^{LLQ} along the line $P_1 = P_2$. Again, the contribution to a_μ is proportional to the volume under the surface as shown. This is shown for the MV and KN form factors in Figs. 8 and 9 respectively. One surprise for us was that while one can see that the tail towards larger values of Q is somewhat larger for the MV form factor than the KN one, it is much less than expected and only marginally visible in the plot. The main conclusion from this section is that the numerical difference between MV and KN comes from relatively low values of Q and moderate values of P_1 and P_2. We have provided plots and numerics so that readers can draw their own conclusions.

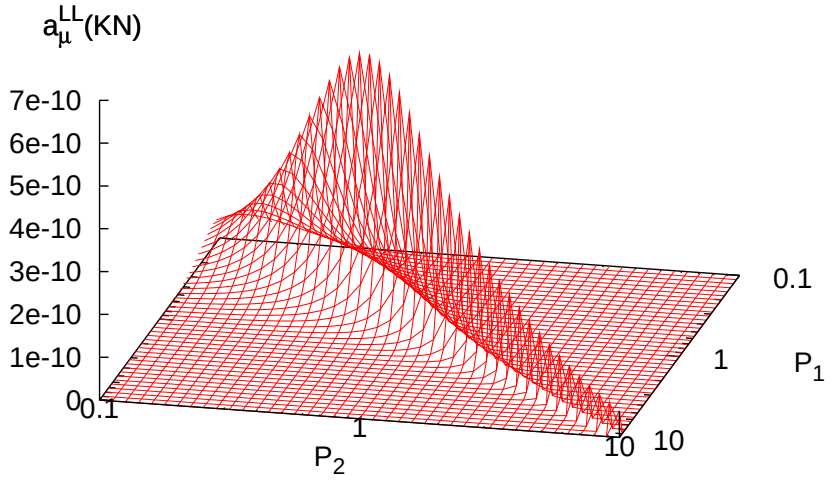

Fig. 6. The quantity a_μ^{LL} of Eq. 10) as a function of P_1 and P_2 for the KN choice. a_μ is directly related to the volume under the surface as plotted.

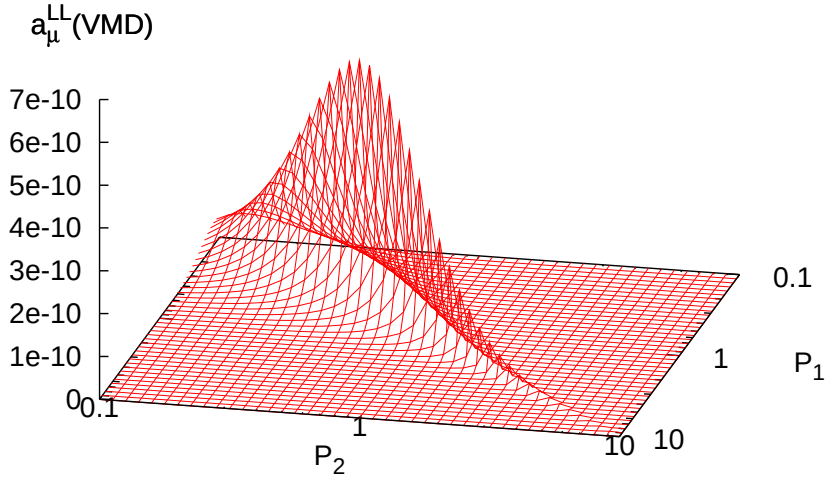

Fig. 7. The quantity a_μ^{LL} of Eq. 10) as a function of P_1 and P_2 for the VMD choice. a_μ is directly related to the volume under the surface as plotted.

5. Comparison

Let us now try to compare the different results of the three calculations in Refs. 8, 13, 10, 14 and 17. In Tab. 7, the results to leading order in $1/N_c$ are shown. The quark loop is of the same order and has to be *added* to get the full hadronic

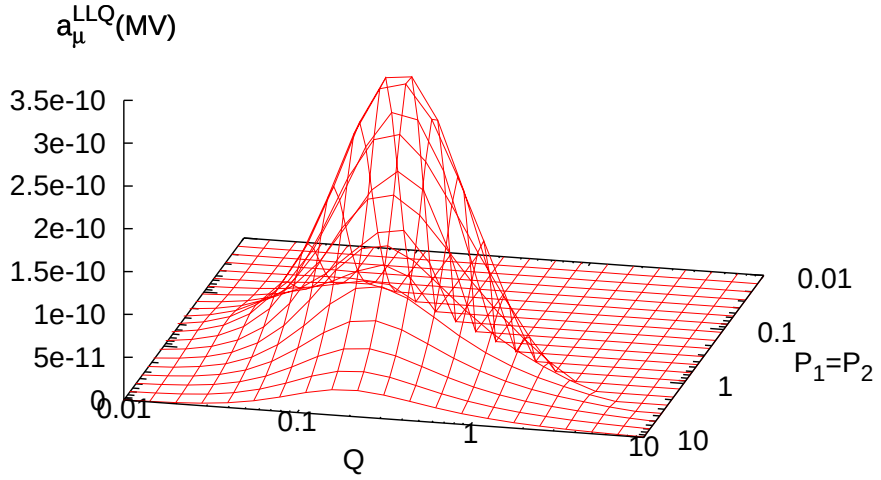

Fig. 8. The quantity a_μ^{LLQ} of Eq. 10) as a function of Q and $P_1 = P_2$ for the MV choice. a_μ is directly related to the volume under the surface as plotted.

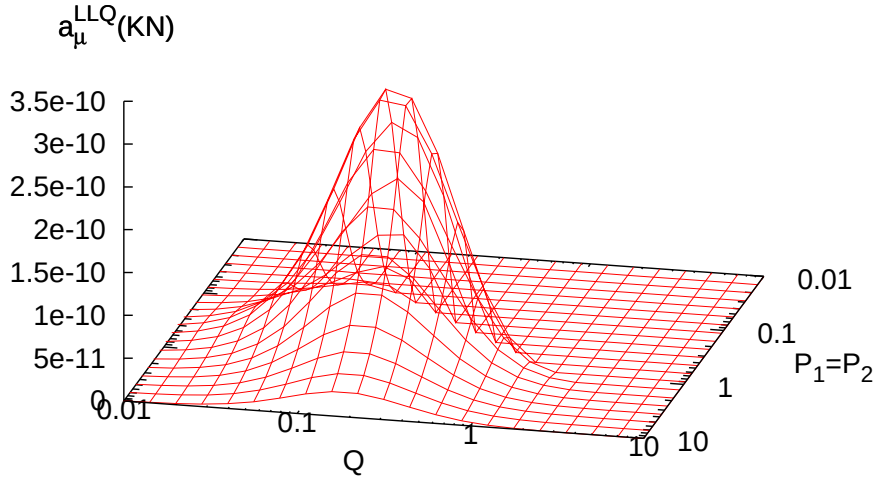

Fig. 9. The quantity a_μ^{LLQ} of Eq. 10) as a function of Q and $P_1 = P_2$ for the KN choice. a_μ is directly related to the volume under the surface as plotted.

light-by-light while the model used in Ref. 17 is saturated just by exchanges. In the GBE the effect of the new OPE in Ref. 17 is a little larger than the quark loop contributions of Refs. 8 and 13 but compatible within one sigma. This contribution has been discussed in more detail in the previous section. The new OPE in Ref. 17

Table 7. Full hadronic light-by-light contribution to a_μ at $\mathcal{O}(N_c)$. The difference between the two results of Refs. 8 and 13 is the contribution of the scalar exchange $-(0.7 \pm 0.1) \times 10^{-10}$. This contribution is not included in Refs. 10, 14 and 17.

Hadronic light-by-light at $\mathcal{O}(N_c)$	$10^{10} \times a_\mu$
Nonet Symmetry + Scalar Exchange [8,13]	10.2 ± 1.9
Nonet Symmetry [8,13]	10.9 ± 1.9
Nonet Symmetry [10,14]	9.4 ± 1.6
New OPE and Nonet Symmetry [17]	12.1 ± 1.0
New OPE and Ideal Mixing [17]	13.6 ± 1.5

similarly increases the axial-vector exchange with nonet symmetry from 0.3×10^{-10} to 0.7×10^{-10} One thus sees a reasonable agreement in the comparison of the $\mathcal{O}(N_c)$ results of Refs. 8, 13, 10, 14 and 17 when using the same mass mixing for the axial-vectors, namely, ($10.9\pm$ 1.9, 9.4 ± 1.6, 12.1 ± 1.0).

The final differences are due to the additional increase of 1.5×10^{-10} from the ideal mixing in the axial vector exchange in Ref. 17 and the scalar exchange of -0.7×10^{-10} in Refs. 8 and 13.

Let us now see what the different predictions at NLO in $1/N_c$ are. In Ref. 17, the authors studied the chiral expansion of the charged pion loop using the HGS model used in Refs. 10 and 14. This model is known not to give the correct QCD high energy behavior in some two-point functions, in particular it does not fulfill Weinberg Sum Rules, see e.g. Ref. 8. Within this model, Ref. 17 showed that there is a large cancellation between the first three terms of an expansion of the charged pion loop contribution in powers of $(m_\pi/M_\rho)^2$. It is not clear how one should interpret this. In Refs. 8 some studies of the cut-off dependence of this contribution were done and the bulk of their final number came from fairly low energies which should be less model dependent. However, it is clear that there is a large model dependence in the NLO in $1/N_c$ contributions. But simply taking it to be $(0 \pm 1) \times 10^{-10}$ as in Ref. 17 is rather drastic and certainly has an underestimated error. The argument of very large higher order corrections when expanded in CHPT orders which was used against this contribution in Ref. 17 also applies to the π^0 exchange as can be seen from Tab. 6 by comparing the WZW column with the others.

Let us now compare the results for the full hadronic light-by-light contribution to a_μ when summing all contributions. The final result quoted in Refs. 8, 13, 10, 14 and 17 can be found in Tab. 8. The apparent agreement between Refs. 8, 13 and 10, 14 final number is hiding non-negligible differences which numerically compensate to a large extent. There are differences in the quark loop and charged pion and Kaon loops and Refs. 10, 14 do not include the scalar exchange.

Comparing the results of Refs. 8, 13 and 17, we have seen several differences of order 1.5×10^{-10}, differences which are not related to the one induced by the new short-distance constraint introduced in Ref. 17. These differences are numerically

Table 8. Results for the full hadronic light-by-light contribution to a_μ.

Full Hadronic Light-by-Light	$10^{10} \times a_\mu$
Bijnens, Pallante and Prades [8,13]	8.3 ± 3.2
Hayakawa and Kinoshita [10,14]	8.9 ± 1.7
Melnikov and Vainshtein [17]	13.6 ± 2.5

of the same order or smaller than the uncertainty quoted in Refs. 8, 13 but tend to add up making the total difference large as follows: The different axial-vector mass mixing account for -1.5×10^{-10}, the absence of scalar exchange in Ref. 17 accounts for -0.7×10^{-10} and the absence of the NLO in $1/N_c$ charged pion and Kaon loops contribution in Ref. 17 accounts for -1.9×10^{-10}. These model dependent differences add up to -4.1×10^{-10} out of the final -5.3×10^{-10} difference between the results in Refs. 8, 13 and 17. In addition we have shown from which regions in momentum the main contribution originates. Clearly, the new OPE constraint found in Ref. 17 alone does not account for the large final numerical difference with respect to Refs. 8, 13 as a reading of it seems to suggest.

6. Conclusions

At present, the only possible conclusion is that the situation of the hadronic light-by-light contribution to a_μ is unsatisfactory. However, looking into the various calculations one finds a *numerical* agreement within roughly one sigma when comparing the $\mathcal{O}(N_c)$ results found in Refs. 8, 10, 13, 14 and 17, see Tab. 7. A new full $\mathcal{O}(N_c)$ calculation studying the full correlator with the large N_c techniques developed in Refs. 22 and 23 and references therein, seems feasible and definitely desirable.

At NLO in $1/N_c$, one needs to control both Goldstone and non-Goldstone boson loop contributions. The high model dependence of the Goldstone boson loop is clearly visible in the different results of Refs. 8, 13 and 10, 14 and discussed in Refs. 8 and 17. For non-Goldstone boson loops, little is known on how to consistently treat them, a recent attempt in another context is Ref. 24.

In the meanwhile, we propose as an educated guess for the total hLBL[e]

$$a_\mu = (11 \pm 4) \times 10^{-10} \,. \tag{11}$$

We believe that, that this number and error capture our present understanding of the hLBL contribution to a_μ. This number can be reached using several different arguments: the new short-distance constraint found in Ref. 17 and the ideal mixing for the axial-vector exchange should lead to some increase of the results of Refs. 8, 13 and 10, 14; the scalar exchange and the pion and Kaon loops are expected to

[e] This educated guess agrees with the one presented by Eduardo de Rafael [3] and ourselves [6] at the "Final Euridice Meeting" in Kazimierz, August 2006 and by one of us (JB) at the "DESY Theory Workshop" in Hamburg, September 2005.

lead to some decrease of the result of Ref. 17; one can also average the leading in $1/N_c$ results (three middle results of Tab. 7) which turn out to be within one sigma. The final error remains a guess but the error in (11) is chosen to include all the known uncertainties.

Acknowledgments

This work is supported in part by the European Commission (EC) RTN network, Contract No. MRTN-CT-2006-035482 (FLAVIAnet), the European Community-Research Infrastructure Activity Contract No. RII3-CT-2004-506078 (Hadron-Physics) (JB), the Swedish Research Council (JB), MEC (Spain) and FEDER (EC) Grant No. FPA2006-05294 (JP), and Junta de Andalucía Grant Nos. P05-FQM-101 and P05-FQM-437 (JP).

References

1. G.W. Bennett *et al.* [Muon $g-2$ Collaboration], Phys. Rev. D **73** (2006) 072003; Phys. Rev. Lett. **92** (2004) 161802.
2. B.L. Roberts [E821 and E969 Collaborations], Nucl. Phys. B (Proc. Suppl.) **155** (2006) 372; Proc. of 6th International Spin Physics Symposium (SPIN 2004), Trieste, Italy, 10-16 Oct. 2004, p. 22-29, hep-ex/0501012.
3. J.P. Miller, E. de Rafael and B.L. Roberts, Rev. Prog. Phys. (to be published); E. de Rafael, Acta Phys. Pol. B (to be published), Proc. of "Final Euridice Meeting", 24-28 August 2006, Kazimierz, Poland.
4. M. Passera, J. Phys. G **31** (2005) R75.
5. M. Knecht, Lect. Notes Phys. **629** (2004) 37 Lectures given at 41st International University School of Theoretical Physics: Flavor Physics (IUTP 41), Schladming, Styria, Austria, 22-28 Feb 2003.
6. J. Bijnens and J. Prades, arXiv:hep-ph/0701240, Acta Phys. Pol. B (to be published), Proc. of "Final Euridice Meeting", 24-28 August 2006, Kazimierz, Poland.
7. M. Hayakawa, T. Blum, T. Izubuchi and N. Yamada, PoS **LAT2005** (2006) 353.
8. J. Bijnens, E. Pallante and J. Prades, Nucl. Phys. B **474** (1996) 379; Phys. Rev. Lett. **75** (1995) 1447 [Erratum-ibid. **75** (1995) 3781];
9. E. de Rafael, Phys. Lett. B **322** (1994) 239.
10. M. Hayakawa and T. Kinoshita, Phys. Rev. D **57** (1998) 465; M. Hayakawa, T. Kinoshita and A.I. Sanda, Phys. Rev. Lett. **75** (1995) 790.
11. M. Knecht, A. Nyffeler, M. Perrottet and E. de Rafael, Phys. Rev. Lett. **88** (2002) 071802.
12. M. Knecht and A. Nyffeler, Phys. Rev. D **65** (2002) 073034.
13. J. Bijnens, E. Pallante and J. Prades, Nucl. Phys. B **626** (2002) 410.
14. M. Hayakawa and T. Kinoshita, Phys. Rev. D **66** (2002) 019902 (Erratum);
15. I. Blokland, A. Czarnecki and K. Melnikov, Phys. Rev. Lett. **88** (2002) 071803.
16. M. Ramsey-Musolf and M.B. Wise, Phys. Rev. Lett. **89** (2002) 041601.
17. K. Melnikov and A. Vainshtein, Phys. Rev. D **70** (2004) 113006.
18. M. Knecht, S. Peris, M. Perrottet and E. de Rafael, JHEP **03** (2004) 035.
19. K. Melnikov, Int. J. Mod. Phys. A **16** (2001) 4591.
20. J. Bijnens and F. Persson, Lund University Master Thesis, hep-ph/0106130.
21. J. Erler and G. Toledo Sánchez, Phys. Rev. Lett. **97** (2006) 161801.
22. J. Bijnens, E. Gámiz, E. Lipartia and J. Prades, JHEP **04** (2003) 055.

23. V. Cirigliano, G. Ecker, M. Eidemüller, R. Kaiser, A. Pich and J. Portolés, Nucl. Phys. B **753** (2006) 139.
24. I. Rosell, J.J. Sanz-Cillero and A. Pich, JHEP **08** (2004) 042.